Chemosphere 194 (2018) 543–552

Contents lists available at ScienceDirect

Chemosphere

journal homepage: www.elsevier.com/locate/chemosphere

Mobility of polivinylpyrrolidone coated silver nanoparticles in tropical soils

Alejandro Yopasá Arenas, Gustavo de Souza Pessôa, Marco Aurélio Zezzi Arruda, Anne Hélène Fostier*

Department of Analytical Chemistry, Institute of Chemistry, University of Campinas, UNICAMP, P.O. Box 6154, 13083-970, Campinas, SP, Brazil

HIGHLIGHTS

- Transport of silver nanoparticles is studied for the first time in tropical soils.
- The on-line monitoring of the surface plasmon resonance produces breakthrough curves.
- Silver nanoparticles have a low retention when transported through the soil columns.
- The behavior of the nanoparticles indicates its potential use as conservative tracer.

GRAPHICAL ABSTRACT

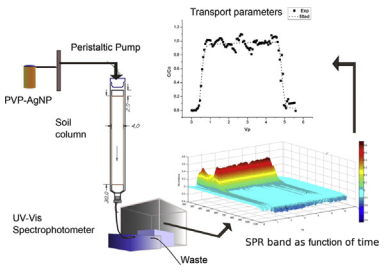

ARTICLE INFO

Article history:
Received 30 August 2017
Received in revised form
28 November 2017
Accepted 4 December 2017
Available online 5 December 2017

Handling Editor: Petra Petra Krystek

Keywords:
Tropical-soil
Transport
Metallic nanoparticles
Silver
UV–Vis
Plasmon

ABSTRACT

Experiments in saturated soil columns were performed to investigate the transport and retention of 25 nm and 75 nm silver nanoparticles stabilized with polyvinylpyrrolidone (PVP-AgNPs) in two Brazilian soils (sandy and sandy-clay). The normalized concentration of the PVP-AgNPs was obtained through a flow injection analysis method based on the surface plasmon ressonance effect of the metallic nanoparticles. The use of the ultraviolet–visible spectroscopy (UV–Vis) allows a rapid and low-cost analysis. The obtained breakthrough curves (BCs) were modeled with a deterministic model of solute transport in steady conditions of water flow and considering two regions of non-physical equilibrium; this model allowed the determination of the hydrodynamic parameters. It was found that the process occurs in condition of non-equilibrium, with a low mass transfer for larger NP, and that the process is predominantly advective and affected by the pore size of the soil packed in the columns. The BCs for PVP-AgNPs obtained by UV–Vis spectroscopy were compared with the BCs obtained by ICP-MS and with BCs of the bromide anion, confirming that the nanoparticles have a low retention and few modifications when transported through the soil column. These PVP-AgNPs are highly mobile and can be transported through the studied tropical soils, representing a potential environmental problem, due to the possibility of these materials reaching groundwater. On the contrary, the conservative behavior of PVP-AgNPs in the studied tropical soils, indicates its potential use as tracers, substituting the bromide anion which has been demonstrated to be not a good tracer in the same conditions.

1. Introduction

The rapid emergence of engineering nanoparticles (ENPs) such as metallic nanoparticles of silver (AgNPs) implies their inevitable

* Corresponding author.
E-mail address: fostier@iqm.unicamp.br (A.H. Fostier).

https://doi.org/10.1016/j.chemosphere.2017.12.019
0045-6535/

appearance in the biosphere. These ENPs suffer large transformations in the environment, which can modify their physicochemical properties, mobility, reactivity and toxicity. It is a critical research question to be able to study under what conditions will ENPs aggregate or disaggregate in relevant environmental media, such as soils (Council, 2013).

The UV–vis spectroscopy can be used for the study of the aggregation behavior of metallic nanoparticles (NPs). The kinetics of aggregation can be determined by measuring the speed at which the absorption band is modified in aqueous solution (Baalousha et al., 2013). The absorption band in the case of metallic nanoparticles is caused by the Surface Plasmon Resonance (SPR) effect; this SPR is the resonant oscillation of the electrons of the conduction band at the interface between a dielectric material and a metal, in response to electromagnetic radiation. SPR is the mechanism responsible for the color of the nanoparticles. Metals such as Au, Ag and Cu show SPR in the visible region of the spectrum. The AgNPs shown a strong SPR at a wavelength of 400–420 nm (Chhatre et al., 2012) with a large molar absorptivity coefficient of $\approx 3 \times 10^{11}$ L mol^{-1} cm^{-1}. The SPR band is dependent on the size, shape, refractive index of the medium, presence of adsorbed species and the aggregation of NP (Prathna et al., 2011; Singha et al., 2014).

For the study of the transport properties of contaminants, the hydrodynamic and the physicochemical contributions are generally separated and the hydrodynamic properties are normally studied with a tracer. In hydrogeology, the term tracer refers to material or energy that can be carried by ground water and gives information concerning the direction and the velocity of the water as well as the potential of transport of contaminants by the water (Ginn and Russel Boulding, 2003). For Davis (Davis et al., 1980) an ideal tracer is neither filtered nor sorbed by the solid matrix through which the water moves (conservative tracer), is inexpensive, easy to detect, it is not present in detectable amounts in the system being studied and is chemically stable for a desired length of time. Studies in the area of transport of contaminants commonly use salts of halogens, mainly KBr, as conservative tracers. The assumption that the Br^- is a conservative tracer for soil-water studies was tested and confirmed for a variety of soils, most of them of temperate regions, and contaminants, including AgNPs (Cornelis et al., 2013; Levy and Chambers, 1987; Sagee et al., 2012; Wang et al., 2015). Nevertheless, in acidic tropical soils, these anionic tracers are not always conservative (Goldberg and Kabengi, 2010). Due to their negative charge, they can be repelled by soil constituents also negatively charged, causing anion exclusion, or can be attracted by positive charges, being adsorbed. Korom and Seaman (2012) summarizes the evidence of the facts pointing out that: Br^- is adsorbed onto Fe and Al oxides and kaolinite (Goldberg and Kabengi, 2010), Br^- adsorption showed no apparent correlation with sediment grain size, and Br^- adsorption is non-linear (concentration-dependent), resulting in greater tailing (hydrodynamic dispersion) than the apparent one for an ideal conservative tracer.

In Brazilian soils, the most frequent minerals (kaolinite, goethite, hematite and gibbsite) have variable charges (Fontes and Weed, 1991; Melo et al., 2001). In these tropical areas the soil is highly weathered and the organic matter content is generally low, due to the high temperatures and high rainfall. These conditions favor the rupture of the primary and secondary mineral structures leading to the formation of simpler compounds such as iron and aluminum oxides and hydroxides. The charges of these compounds are pH dependent, and in the acidic Brazilian soils (IGBP-DIS, 1998) these oxides and hydroxides will have a positive surface charge, able to retain anions such as the Br^-. These Fe and Al oxides can also be the main surface for ionic exchange, and then, depending of the pH, the anion capacity exchange can surpass the cation exchange capacity (Fontes and Alleoni, 2006).

As for Br^-, it can therefore be expected that the transport of some contaminants, such as AgNPs, can be affected in such tropical Brazilian soils. According to Kumahor (Kumahor et al., 2016), the transport of AgNPs is particularly sensitive to pH and to the concentration of multivalent cations in soil solution. Wang (Wang et al., 2015) also found that pH, cation exchange capacity (CEC), soil organic matter content and type, Fe oxide content and specific surface area control the fate and transport of polyvinylpyrrolidone-coated silver nanoparticles (PVP-AgNPs). The aim of this work was, therefore, to study the transport properties of PVP-AgNPs in two tropical soils. For this purpose, a simple UV–Vis based spectrophotometric analytical method was also proposed.

2. Materials and methods

2.1. Chemicals and analytical methods

PVP-AgNPs, were acquired in form of dispersion (5 mg Ag mL^{-1}) from Nanocomposix, Inc. 75 nm PVP Econix Silver, Lot Number: DAC1270, diameter (TEM): 74.5 ± 11.8 nm, coefficient of variation: 15.9%. 25 nm PVP Econix Silver, Lot Number: DAC1610, diameter (TEM): 23.1 ± 6.9 nm, coefficient of variation: 29.8%. Other reagents used were KBr and $NaNO_3$ (ACS, Mallinckrodt), methylene blue (P.A. Labsynth), H_2SO_4 (P.A. ACS, Merck), 30% H_2O_2 and HNO_3 (ISO, Merck).

The UV–Vis spectra were obtained by using an Agilent 8453 UV–Vis spectrophotometer with a flow cell of quartz, 2 mm round aperture, M6 thread, 10 mm of path length, and 30 μL volume. The propulsion of the solutions into the soil column was provided by a multichannel Ismatec® peristaltic pump model IPC, and Tygon® tubing with an inside diameter of 1/18 inch. The real density was determined in a gas picnometer ULTRAPYC 1200e (Quantachrome Instruments). The quantitation of silver was carried out by using an inductively coupled plasma mass spectrometer (ICP-MS) model Elan DRC (PerkinElmer) equipped with a quadrupole analyzer and a dynamic reaction cell. The operating conditions of the equipment are reported in Table 1. The decomposition of soil samples was performed in a microwave oven DGT100 Plus (Provecto Analytics, Jundiaí, Brazil) equipped with temperature sensor and magnetron of 2450 ± 13 MHz with nominal power of 1200 W was used.

Silver was quantified by ICP-MS in fifteen samples (2 mL each) of soil column eluates (3 columns for each soil type), in order to confirm the data obtained by the spectrophotometric method. The digestion of the eluted PVP-AgNPs solutions was carried out in a microwave oven. 25 μL of sample was placed in a PTFE reactor with 2.0 mL of HNO_3 (65%) and 0.5 mL of H_2O_2 (33%) and it was applied an heating program in four steps: 5 min-400 W/8 min-790 W/4 min-320 W and 3 min-0 W. Then, the digested samples were diluted to 25.0 mL with ultra pure water for posterior analysis by ICP-MS.

In order to determine the concentration of silver retained in soil, one soil column for each soil type was sliced every 5 cm, homogenized and dried at 120 °C for 24 h. Subsequently, three 150 mg subsamples of each column fraction were submitted to a total digestion by microwaves by placing the samples in a closed PTFE reactor with 2.7 mL of HNO_3 (65%), 0.3 mL of H_2O_2 (33%), and 0.45 mL of HF (40%). A five steps heating program was then applied: 3 min-250 W/5 min-500 W/5 min-600 W/5 min-700 W and 2 min-80 W. After decomposition, the extracts were treated with 5 mL of 5% H_3BO_3 solution and heated for 5 min at 100 °C to allow fluorine complexation. Finally, the solutions were transferred to a 25.0 mL Falcon R flask and diluted to the mark with MilliQ® water.

Table 1
Operating conditions of the ICP-MS equipment for the analysis of silver in eluate samples.

Equipment	PerkinElmer Elan DRC-e
Nebulizer chamber	Ciclonic
Nebulizer	Concentric
Potency RF (W)	1200
Nebulizator gas flow (Ar, L min^{-1})	0.79 (optimized daily)
Auxiliary gas flow (Ar, L min^{-1})	1.23
Plasm gas flow (L min^{-1})	15.00
m/*z*	$^{107}Ag^{+}$
Detector dead time (ns)	60
Replicates	3
Detector mode	Dual
Lecture mode	Peak hoping
Sweeps	20
Residence time (ms)	50
Integration time (ms)	3000

2.2. Soil Samples

A dystrophic Red-Yellow Latosol (LVAd) and an Ortic Quartzarenic Neosol (RQo) according to the Brazilian Soil Classification System (SiBCS). The LVAd soil was collected in a forested area located in the Campinas municipality, (22°51′28″ S and 47°05′56″ W), the RQo soil was collected in the municipality of São Pedro, (22°33′53″ S and 47°52′06″ W). Both sample points are located in São Paulo (Southeast Brazil) and can be considered as non-directly impacted by anthropic activity. The samples were taken at depth of 0–20 cm; sieved on a 2 mm mesh and dried at room temperature. Physicochemical properties of soils are presented in Table 2.

2.3. Packaging of the soil and washing of the column

By working under conditions of non-equilibrium in a soil column it was possible to assess a more realistic experimental conditions when compared to the equilibrium conditions of batch experiments (OECD, 2000). Glass column of 34 cm long and 4 cm of inner diameter, with two baffle zones made of glass wool (2 cm each), was prepared as recommended by Barry (2009) for a uniform unidirectional flow. The column design has been improved when compared to other recent used in studies of AgNP mobility in soils (Cornelis et al., 2013; Sagee et al., 2012). The deflector zones assure a steady unidirectional flow conditions required by the transport model used in the present study. The column design meets the recommendations of the Organization for Economic Co-operation and Development for leaching studies (OECD, 2004). For packaging, small amounts of wet soil were deposited in the glass column filled with deionized water under manual agitation to achieve a uniform and dense packing (Oliviera et al., 1996). For the sandy-clay LVAd soil 340 ± 5 g d.w. (mean ± sd, n = 4) were packed; for the sandy soil RQo 456 ± 10 g d.w. (mean ± sd, n = 4) were packed. The soil column was then washed with 10 pore volumes (PV) of sodium nitrate solution (0.05 mg mL^{-1}) in a down-flow mode.

Table 2
Physicochemical properties of the studied soils.

Variable	Method	Unit	Soil	
			LVAd	RQo
pH	$CaCl_2$ 0.01 mol L^{-1}		4.4	4.0
OM	Colorimetric	g L^{-1}	34	13
P	Resin	mg L^{-1}	8	3
K	Resin	mmolc L^{-1}	1.1	0.1
Ca	Resin	mmolc L^{-1}	13	1
Mg	Resin	mmolc L^{-1}	5	0
Na	CH_3COONH_4 pH 7	mmolc L^{-1}	0.1	0.1
Exchangeable Al	KCl 1 mol L^{-1}	mmolc L^{-1}	2	5
Exchangeable Al + H	SMP buffer	mmolc L^{-1}	46	23
Base sum	Calculated	mmolc L^{-1}	19.2	1.2
CEC	Calculated	mmolc L^{-1}	65.2	24.2
Base saturation	Calculated	%	29	5
S as SO_4^{2-}	$Ca(H_2PO_4)_2$	mg L^{-1}	6	3
B	Hot water	mg L^{-1}	0.28	0.11
Cu	DTPA pH 7.3	mg L^{-1}	4.3	0.3
Fe	DTPA pH 7.3	mg L^{-1}	47	53
Mn	DTPA pH 7.3	mg L^{-1}	7.6	1.1
Zn	DTPA pH 7.3	mg L^{-1}	1.5	0.7
Sand	Pipette/hydrometer	%	50.9	93.2
Silt	Pipette/hydrometer	%	8.2	1.5
Clay	Pipette/hydrometer	%	40.9	5.1
Texture	USDA		Sandy-Clay	Sandy
Superficial Area	BET	m^2 g^{-1}	47.221	28.882
Real Density	He picnometer	g cm^{-3}	2.6614	2.6956
Porosity	Calculated		0.66	0.55

2.4. Bromide transport experiments in soil columns

The bromide anion that percolated the column was detected by flow injection analysis (FIA) system coupled to a soil column as represented in Fig. 1. Three columns of each soil type were prepared and one breakthrough curve (BC) was obtained from each column. The method is based on the catalytic effect of bromide in the oxidation of methylene blue by hidrogen peroxide in acidic media (Uraisin et al., 2006; Zaribafan et al., 2014). Experimental details of the developed method are presented in the Supplementary material (SM).

2.5. Nanoparticles transport experiments in soil columns

To resuspend the settled nanoparticles the bottles were vigorously shaken to a homogenous dispersion (typically ~ 30 s). The diluted dispersion was prepared by diluting 1.00 mL of the 5000 mg L^{-1} PVP-AgNP dispersion to 1000.0 mL with Milli-Q water. The stability of the dispersion was monitored by UV–Vis for 30 h (see Fig. 5 of the SM). The maximum of the SPR band does not change during this time, which ensures the stability of the diluted PVP-AgNP dispersion for a time that is approximately 3 times longer than the transport experiment.

Nanoparticles transport experiments were carried out directly coupling the column to the UV–Vis spectrophotometer by means of a continuous flow cell (Fig. 2). A peristaltic pump was used to percolate nanoparticles dispersion at a constant volumetric flow (Q = 3.1 mL min^{-1}) through the column. Three columns of each soil type were prepared and one BC was obtained from each column. The soil column was initially percolated with four pore volumes of PVP-AgNPs dispersion (5.0 mg L^{-1}), followed by the eluent solution (sodium nitrate 0.05 mg mL^{-1}). Spectra of the eluted solution were collected every 30 s for 7.5 h, monitoring the wavelength of maximum absorption (398 nm for 25 nm nanoparticles and 450 nm for 75 nm nanoparticles). The BC was obtained from the response surface, assuming that C/Co = A/Ao (Beer Law). C_0 corresponds to the initial concentration of the PVP-AgNPs dispersion (5.0 mg L^{-1}), C is the concentration over percolation time. A_0 corresponds to the height of the plasmon band (or maximum absorbance) of a 5.0 mg L^{-1} PVP-AgNPs dispersion, A is the maximum absorbance of the plasmon band over percolation time. The construction of the BC was then simplest by using A/Ao in state of C/Co. As absorption reading is automatically done in the online system, this is a quick and simple way of obtaining the BC.

2.6. Nanoparticule transport modelling

Transport parameters were estimated by the evaluation of

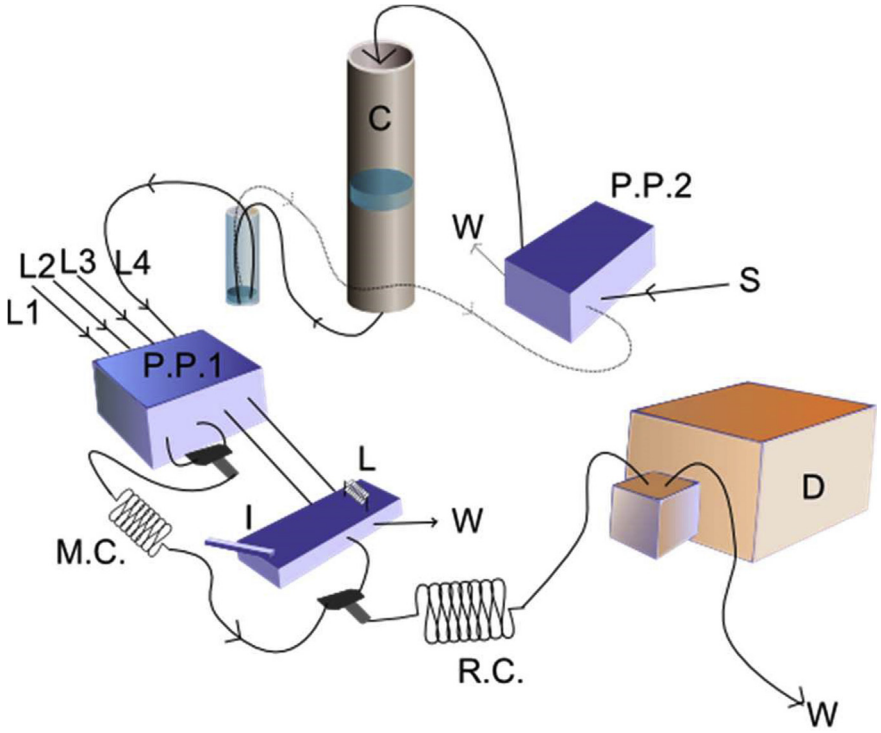

Fig. 1. Flow injection system (FIA) used for bromide determination. S: 3.0 mg mL^{-1} Br^{-} solution, P.P.: peristaltic pump, C: soil column, W: waste, L1: H_2O_2 1.6%, L2: methylene blue 8.0×10^{-5} mol L^{-1} in H_2SO_4 2.5 mol L^{-1}, L3: Water, L4: column eluate, M.C.: mixing coil, I: Injector, L: 800 μL sample loop, R.C: reaction coil, D: Detector (spectrophotometer UV–Vis). (For interpretation of the references to color in this figure legend, the reader is referred to the Web version of this article.)

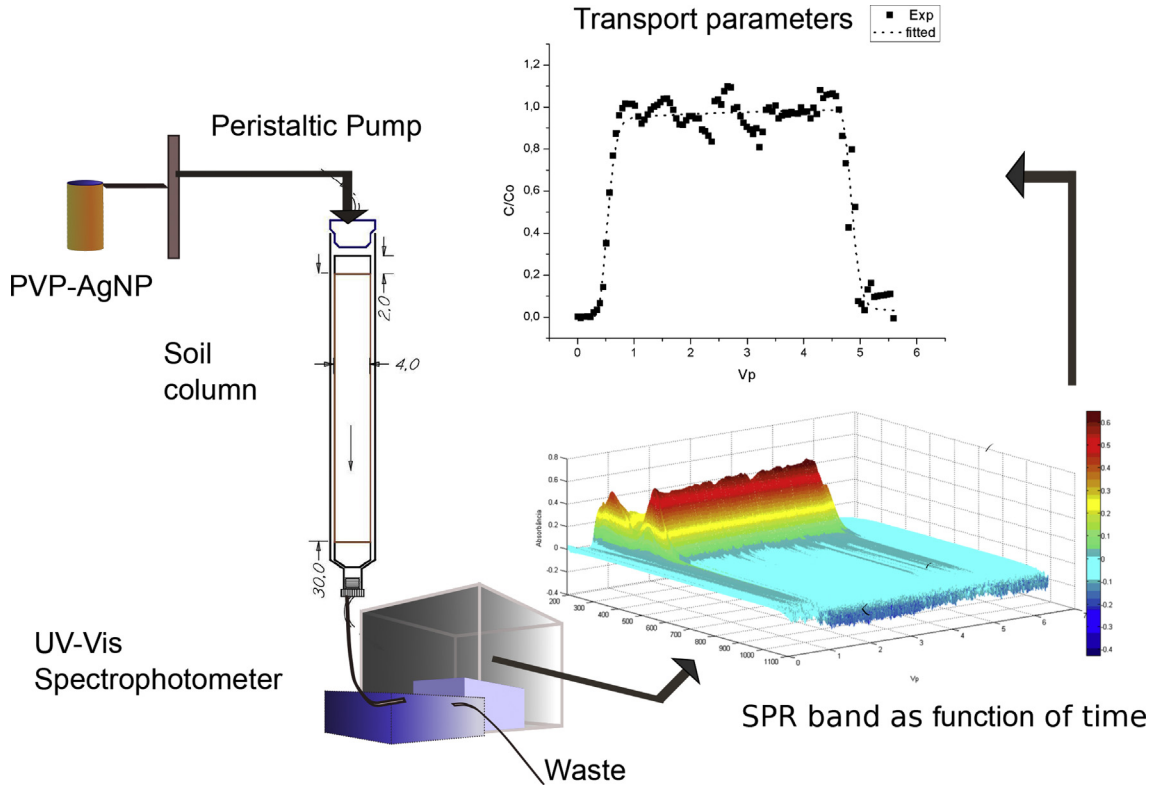

Fig. 2. Experimental setup that describes the obtaining of the breakthrough curves from Uv–Vis data in an on-line system.

analytical solutions of the advection-dispersion equation (ADE). An inverse optimization method was applied by using the numerical code CXTFIT included in the STANMOD software V. 2.08 (Šimůnek et al., 2008). It was chosen a deterministic model of solute

transport in steady conditions of water flow, considering two regions of physical nonequilibrium. In this representation the liquid phase is divided into two regions, mobile (predominantly advective flow) and immobile (stagnant) (Simunek et al., 2006). This approach is the simplest representation of a transport process in non-equilibrium conditions. The dimensionless representation of the model is given by equations (1a) and (1b).

$$\beta R\frac{\partial C_I}{\partial T}+(1-\beta)R\frac{\partial C_{II}}{\partial T}=\frac{1}{P}\frac{\partial^2 C_I}{\partial X^2}-\frac{\partial C_I}{\partial X} \quad (1a)$$

$$(1-\beta)R\frac{\partial C_{II}}{\partial T}=\omega(C_I-C_{II}) \quad (1b)$$

where C_I and C_{II}: dimensionless concentration in the mobile and the immobile regions, respectively; T: dimensionless time (also known as pore volume or column porosity); X: dimensionless distance; P: Peclet number; ω: dimensionless mass transfer coefficient; R: retardation factor; β: partitioning coefficient.

3. Results and discussion

3.1. Breakthrough curves of bromide in soil columns

The optimized FIA system parameters, for degradation of methylene blue with H_2O_2 catalyzed by Br^- ion were: injection loop volume = 800 μL; mixing coil volume = 4000 μL, flow rate (H_2O_2, Br^- and methylene blue lines) = 0.5 mL min^{-1}, methylene blue concentration = 8.0 × 10^{-5} mol L^{-1} in H_2SO_4 2.5 mol L^{-1}, concentration of bromide ion = 0–3 mg mL^{-1}, wavelength = 664 nm. Measurements of three distinct curves were performed on different days to measure the reproducibility of the system. From the covariance analysis (ANCOVA) it was concluded that the calibration curves can be described by the same linear regression ($p<0.05$) with an angular coefficient of 3.24 ± 0.28 (Absorbance unit mol^{-1}) and an intercept of 0.26 ± 0.22 (Absorbance unit).

The breakthrough curves presented in Fig. 3 show that bromide does not behave as a conservative tracer in the two soils. The asymmetry and the long tail are indicators of non-linear adsorption and anion exclusion. The absorption of bromide on amorphous Al and Fe oxides, kaolinite and monrmorillonite was verified by Goldberg and Kabengi (2010). These components are generally part of tropical soils (Fontes and Alleoni, 2006; Fontes and Weed, 1991) and the adsorption of Br^- can therefore be expected.

3.2. Breakthrough curves of PVP-AgNP percolated in soil columns

Each breakthrough curve (BC) of PVP-AgNPs was obtained from a matrix dataset, corresponding to the UV–Vis spectra of PVP-AgNPs as a function of time. An example of one data set is shown in Fig. 4. In this case, the maximum and width of the SPR band are constant, indicating that PVP-AgNPs did not suffer any type of interaction with soil, nor aggregation or decomposition. The small band observed at 380–400 nm corresponds to dissolved organic matter (see the total organic carbon profile and fluorescence analysis in SM, Figs. 6 and 7).

The experimental breakthrough curves for both soil types and both sizes of nanoparticles are shown in Fig. 5. The BCs of PVP-AgNPs are more symmetrical and sigmoidal than the BCs obtained for bromides. The symmetry of the curves shows that it does not exist a significant interaction of PVP-AgNPs with the soil matrix. The PVP-AgNPs can therefore be considered as conservative tracers for the two types of studied soils. The breakthrough curves show similarity with the retention profiles of PVP-AgNP obtained by Wang (Wang et al., 2015) in loam (Hapli-Stagnic Anthrosol) and sandy-loam (Usti-Alluvic Primosol) soils, for nanoparticles suspended in 1 mmol L^{-1} KNO_3, or 0.5 mmol L^{-1} $Ca(NO_3)_2$".

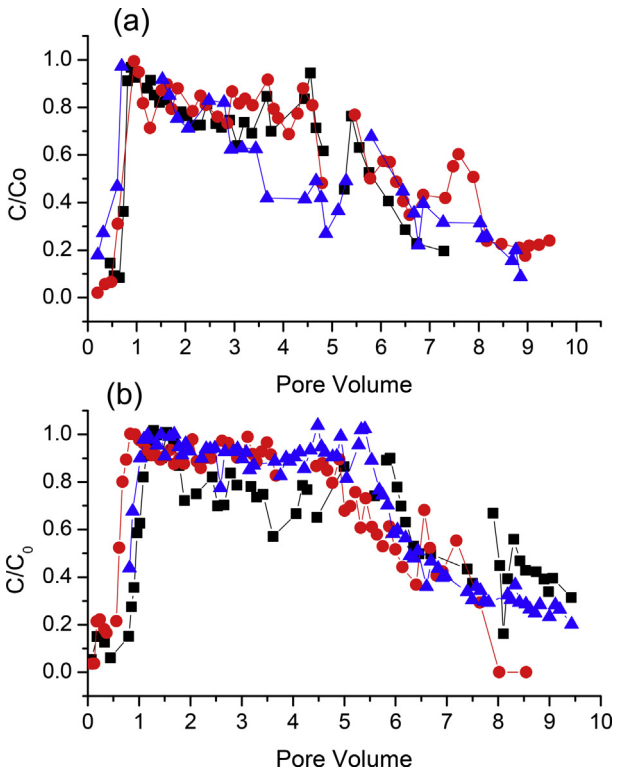

Fig. 3. Breakthrough curves for bromide in the two tropical soils, a) sandy soil RQo and b) clay soil LVAd (each curve obtained in triplicate: ▲,○,□).

The parameters of the BCs obtained from the code CXTFIT are shown graphically in Fig. 6 (the numerical data obtained from stanmod are in Table 1 of the SM). The mass transfer process occurs as a result of the movement of the nanoparticles themselves and is defined by the Fick's first law which establish that the amount of matter that diffuses at a time t, through a surface perpendicular to the diffusion direction, is proportional to the concentration gradient of the substance that diffuses. The diffusion coefficient (D_d) represents the amount of matter that is diffused per unit of

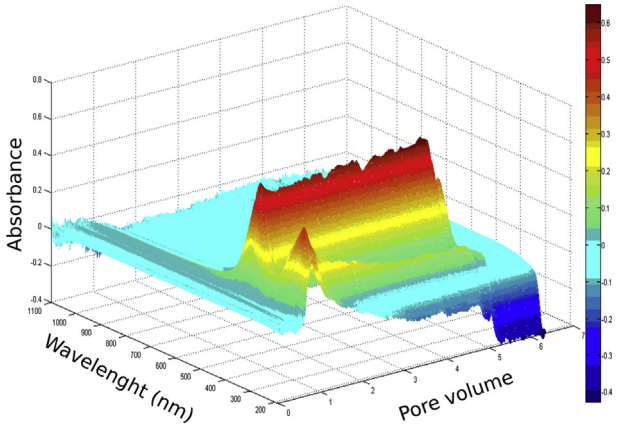

Fig. 4. Surface response of the Uv–Vis spectra of 75 nm PVP-AgNPs, eluted from a sandy-clay soil column, as a function of dimensionless time (pore volume). The structure of the surface responses was similar for the 25 and 75 nm PVP-AgNPs for both soils. The maximum of the SPR is at 450 nm for 75 nm PVP-AgNPs and 398 nm for 25 nm PVP-AgNPs.

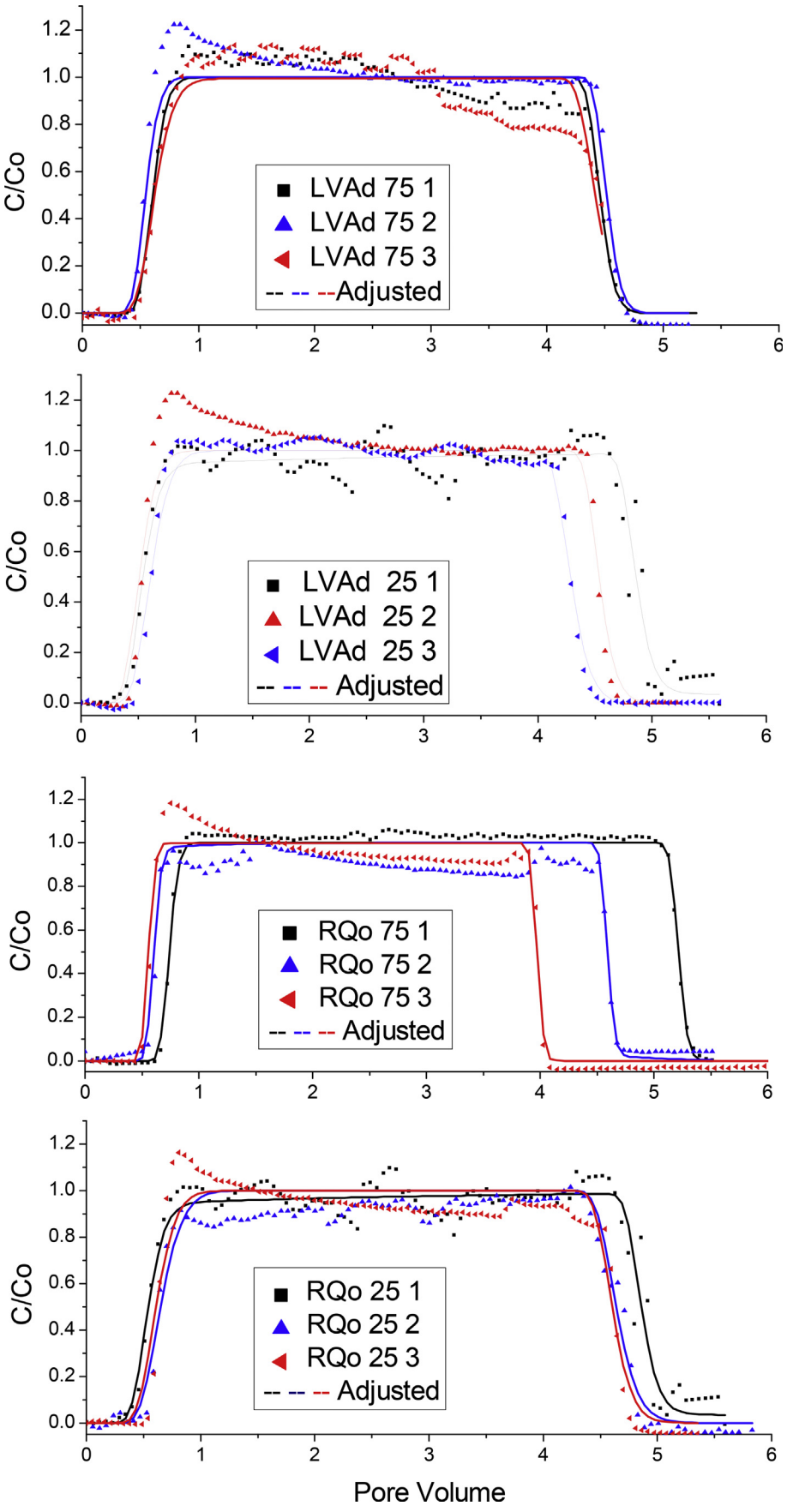

Fig. 5. Breakthrough curves of 25 and 75 nm PVP-AgNPs in both soils. Sandy soil (RQo) and clay soil (LVAd).

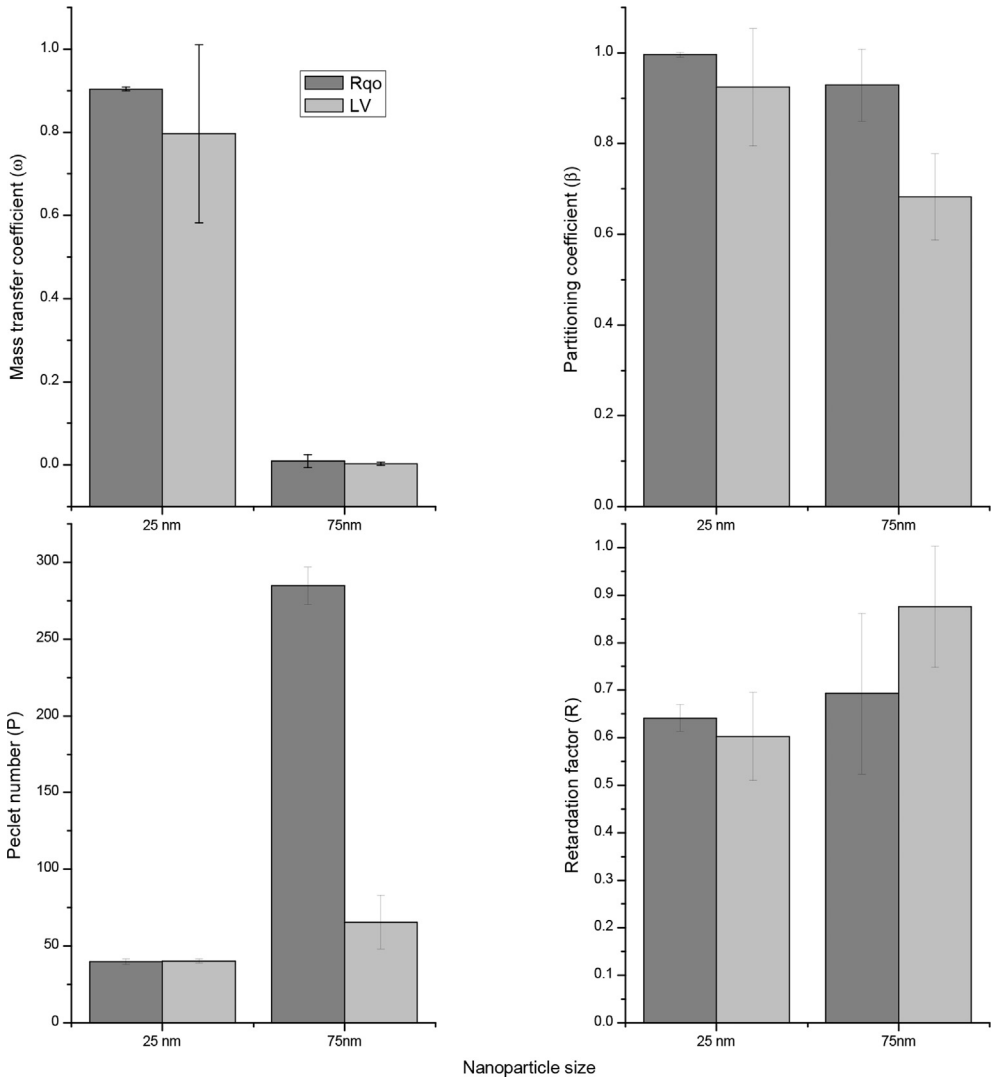

Fig. 6. Parameters of the breakthrough curves of PVP-AgNP obtained from the code CXTFIT. For two sizes of nanoparticles (25 and 75 nm) and two types of soils (clay: LVAd, sandy: RQo). ω: dimensionless mass transfer coefficient, β: partitioning coefficient, P: Peclet number, R: retardation factor.

time through the surface unit when the concentration gradient is equal to 1. These diffusion coefficient values depend on the properties of the diffusing nanoparticles and also on the properties of the medium in which it diffuses. Since the mass transfer coefficient (ω, $0 < \omega < 1$) is directly proportional to the diffusion coefficient (Maraqa, 2001), the relatively low value of ω in sandy and clay soil for 75 nm nanoparticles indicates a low NP transfer between the mobile-immobile water regions, closely analogous to a diffusive process. From the point of view of kinetic-molecular theory, this is an expected result since larger particles have lower diffusion rates. Thus, larger nanoparticles have greater difficulty in moving in the medium which can be understood as the boundary between the mobile and immobile water regions (Selim and Amacher, 1997).

The partition coefficient between the mobile and immobile water region (β), also called non-equilibrium coefficient, may have values between zero and one. Zero indicates a total non-equilibrium condition and one indicates a total equilibrium condition between the two regions. In the model there is an immobile region that corresponds to the water that is retained inside the pores on the surfaces of the solid material, and a mobile region that corresponds to the water that moves freely along the pores due to the water-potential gradient (Yaron et al., 1973). Fig. 6 shows that the partition coefficient β is affected by the size of the nanoparticles for the two types of soils. β values for 75 nm nanoparticles are lower when compared to the 25 nm nanoparticles in the two soil types. This difference indicates that it is easier for the 25 nm PVP-AgNPs to establish the dynamic partition equilibrium between regions at the flow velocity established in the experiment (3.1 mL min^{-1}). This result can be explained by the fact that the smaller nanoparticles have a greater hydrodynamic dispersion and, therefore, they will take less time in the process of entry and exit of the pores-water regions. The partition process may also be affected by the size and type of pores (the smaller the pore size the greater the amount of immobile water), the structural properties of the column and the type of water retention processes (Nimmo, 2004).

The Peclet number (P) is a parameter that measures the predominance of the advective process over the diffusive process (Rosas Medina, 2005), P can be described by equation (2) (van Genuchten and Leij, 2001):

$$P = \frac{Vd}{D_d} \tag{2}$$

where V is the mean flux rate, d is the average grain diameter and

D_d is the diffusion coefficient. D_d is a macroscopic coefficient that accounts for several mechanisms such as molecular diffusion and mechanical dispersion of the particles during transport. For flow velocities such as those used in this work it can be assumed that the main contribution to the dispersion comes from the mechanical dispersion (Brusseau, 1993). The mechanism of mechanical dispersion (F_H) is expressed by Equation (3) (Selim and Amacher, 1997):

$$F_H = -\theta D_H \frac{\partial C}{\partial z} \quad (3)$$

where D_H is the mechanical dispersion coefficient, C is the concentration and z is the direction. For the 25 nm PVP-AgNPs it was observed a smaller Peclet number when compared to 75 PVP-AgNPs in both soils (Fig. 6), the difference indicates the importance of the dispersive over the advective component. The 25 nm PVP-AgNPs are more easily dispersed than the 75 nm PVP-AgNPs because they are smaller and lighter and suffer less resistance in their passage through the soil pores. The smallest nanoparticles are also more delayed than the largest nanoparticles because they can entry into pores where the nanoparticles of 75 nm do not. These smallest nanoparticles are also more affected by the variations (on both direction and magnitude) of the relative velocity of the fluid elements caused by the variations on the pore radius (Nimmo, 2004). NP size poorly affects P value in the clay soil. This can likely be explained by the fact that the clay soil is a low permeability environment; in this soil only a fraction of the total water-filled porosity (reported in Table 2) is available for dispersion transport, so the effects of pore and water velocity are less pronounced than in the sandy soil (Huysmans and Dassargues, 2005).

The retardation factor R indirectly expresses the soil's capacity to retain the PVP-AgNPs; R is assumed to be related to the solute adsorption distribution coefficient k (Li and Shuman, 1997). In the sandy soil no significant difference was observed between the R values of both sizes particles (Fig. 6), when for the clay soil R tend to increase for the largest particles. The clay soil contains higher clay and organic matter contents; both components in which distribution of PVP-AgNPs can be expected (Table 2). On the other hand, in the sandy soil the composition should not affect the retardation of NPs of different sizes; Li and Shuman (1997) also reported that the adsorption is generally more linear on sandy soils than on clay soils. Adsorption of PVP-AgNPs by ionic interactions on charged soil particles (mainly clay) are also unexpected, because the PVP-AgNPs are uncharged particles. The retardation factor R is less than one for both soils and both nanopaticles sizes; this indicates that only a fraction of the liquid phase participates in the transport process. This occurs when immobile liquid regions are present but do not participate in the convective transport process, for example, water in fine-pores (micro and cryptopores), water retained within dense aggregates or away from saturated macropores (Nimmo, 2004; Osman, 2013).

3.3. Comparison with mass spectrometry

The proposed method presents a limit of detection (LD) of 0.05 $\mu g\ L^{-1}$ ($LD = x_0 + 3S_0$ with $n = 20$) and a limit of quantification (LQ) of 0.09 $\mu g\ L^{-1}$ ($LQ = x_0 + 10S_0$ with $n = 20$), the correlation of the quantized curve is linear and can be expressed as Intensity = 16709 × Ag concentration. The method is thus suitable for the determination of low concentrations of silver, such as those found in eluates from the leaching experiment and in the soil

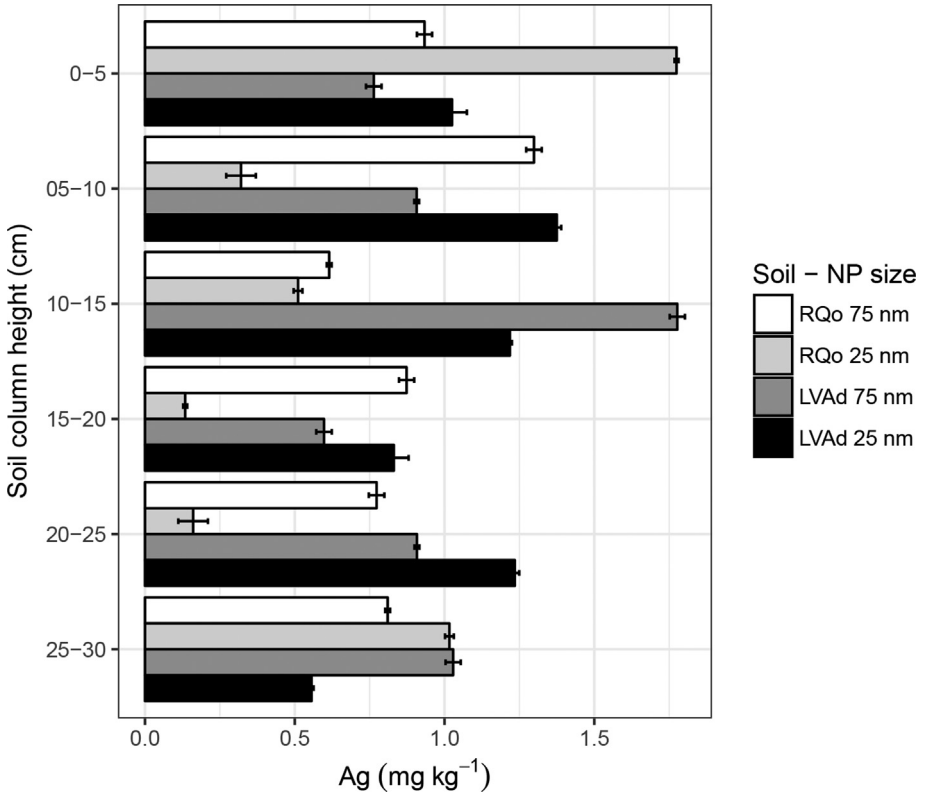

Fig. 7. Concentration of silver obtained from ICP-MS data as a function of depth along the soil column for sandy (RQo) and clay (LVAd) soils and for both PVP-AgNPs 25 and 75 nm sizes.

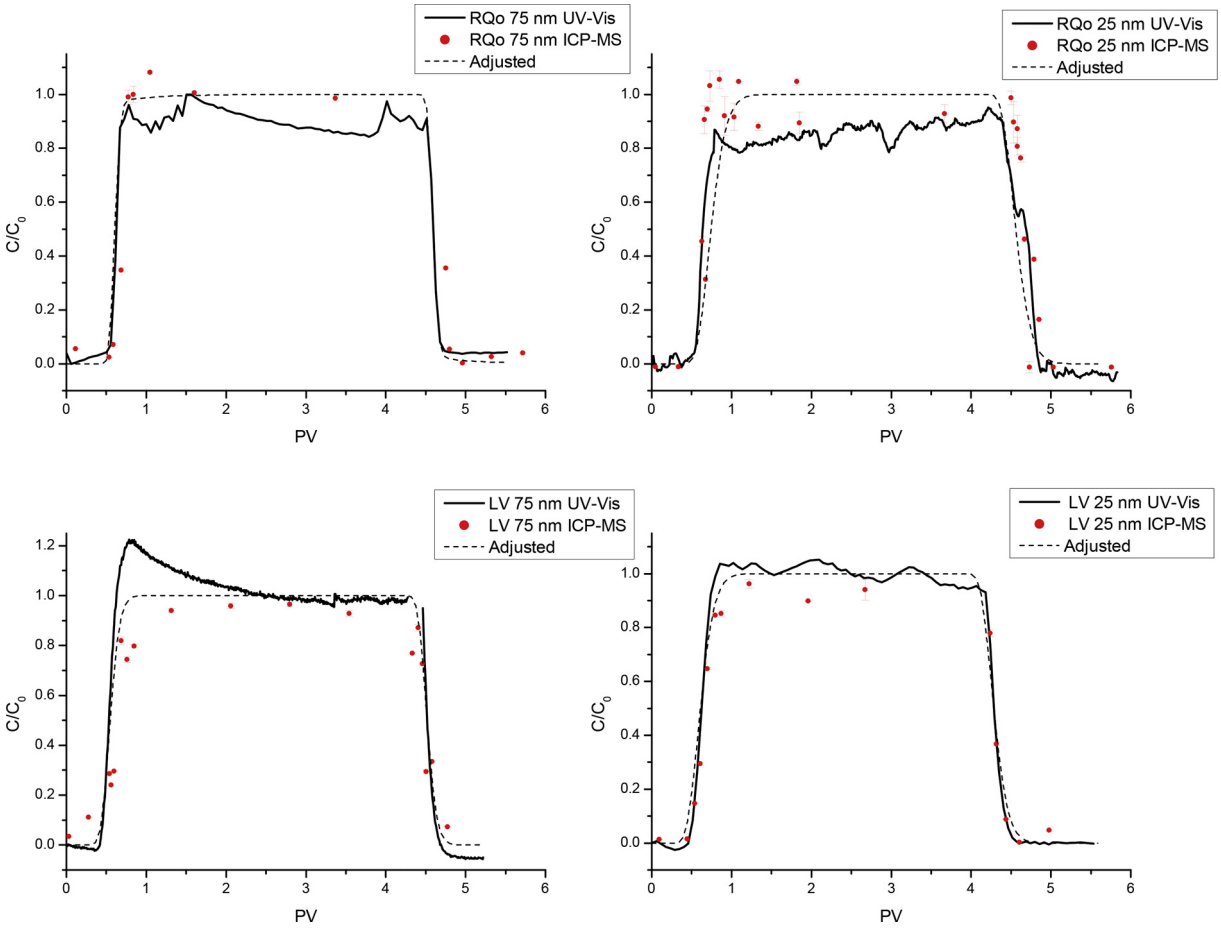

Fig. 8. Comparison between the breakthrough curves obtained by monitoring of the plasmon band (UV–Vis) and those obtained from quantitation of silver by ICP-MS, PV: Pore Volume, error bars represent the standard deviation.

column. Determination of silver by ICP-MS is a slower process compared with the UV–Vis method due to sample preparation and analysis, but it allows obtaining information on the amount of Ag sorbed in the soil solid matrix. The Ag concentrations (mg kg^{-1}) along the soil column after subtraction of blank values are reported on Fig. 7. The concentration of Ag retained on each soil slice was always lower than 2 mg kg^{-1} and the total amount of Ag retained in the entire column was always lower than 10% when compared to the total amount of silver percolated in the soil column. These data show the low retention of PVP-AgNPs in both soils. The 25 nm PVP-AgNPs were more retained in the upper part of the sandy soil column (RQo, 0–5 cm), whereas the 75 nm NPs were more retained in the central part of the clay column (LVAd, 10–15 cm). A more uniformed distribution along the columns was observed for 75 nm NPs in the sandy soil and for 25 nm NPs in the clay soil.

As shown in Fig. 8, breakthrough curves obtained by measuring the plasmon fit well with those obtained by determining the total silver concentration by ICP-MS in selected eluate samples. These data confirm that PVP-AgNPs are weekly retained in both soils. Nevertheless, the UV–Vis measurements present some differences in the case of nanoparticles transported in the clay soil (Fig. 8 - LVAd 75 nm); in this and other breakthrough curves (Fig. 5), a peak appears in the region close to a pore volume of 1. The presence of this type of readings ($C/C0 > 1$) can be explained by the absorption of the dissolved organic matter (DOM) co-transported with the PVP-AgNPs. In the ICP-MS breakthrough curves this peak is not observed, likely due to the degradation of the organic matter in the digestion process of the samples.

4. Conclusions

The flow injection analysis system (FIA) used for the determination of AgNPs in eluates, coupled to a soil column enables the realization of the experiments in a relatively short time, allowing the analysis of a larger number of samples and with lower cost due to the required instrumentation. When comparing the results of the bromide with those of the PVP-AgNPs, one can conclude that these latter behave as a conservative tracer. This means that PVP-AgNPs do not strongly interact with the soil matrix and have a high mobility, which can lead to an environmental problem because of the groundwater contamination. On the other hand, as it was shown that PVP-AgNPs present a conservative behavior in tropical soils, they could be used for transport studies of other types of contaminants, substituting the bromide which has been demonstrated to be not a good tracer in the studied soils.

Breakthrough curves obtained by monitoring the plasmon band are easier to obtain and avoid sample preparation steps, such as required for nanoparticle digestion for silver determination by ICP-MS. Although the rupture curves obtained by UV–vis spectroscopy were similar to those obtained by total silver determination by ICP-MS, in the latter, baseline problems observed in the plasmon band due to the soil organic matter are corrected. This suggest the complementary of both techniques in the studies of metallic nanoparticles in environmental matrices.

Acknowledgements

National Council of Technological and Scientific Development – CNPQ (process number 153585/2013-7). São Paulo Research Foundation - FAPESP (grant number 2016/07384-7). Coordination for the Improvement of Higher Education Personnel - CAPES (process number 88881.062204/2014-01). National Institute of Science and Technology for Bioanalytics (INCTBio).

Appendix A. Supplementary data

Supplementary data related to this article can be found at https://doi.org/10.1016/j.chemosphere.2017.12.019.

References

Baalousha, M., Nur, Y., Römer, I., Tejamaya, M., Lead, J.R., 2013. Effect of monovalent and divalent cations, anions and fulvic acid on aggregation of citrate-coated silver nanoparticles. Sci. Total Environ. 454–455, 119–131. https://doi.org/10.1016/j.scitotenv.2013.02.093.

Barry, D.A., 2009. Effect of nonuniform boundary conditions on steady flow in saturated homogeneous cylindrical soil columns. Adv. Water Resour. 32, 522–531. https://doi.org/10.1016/j.advwatres.2009.01.003.

Brusseau, M.L., 1993. The influence of solute size, pore water velocity, and intraparticle porosity on solute dispersion and transport in soil. Water Resour. Res. 29, 1071–1080. https://doi.org/10.1029/92WR02595.

Chhatre, A., Solasa, P., Sakle, S., Thaokar, R., Mehra, A., 2012. Color and surface plasmon effects in nanoparticle systems: case of silver nanoparticles prepared by microemulsion route. Colloids Surfaces A Physicochem. Eng. Asp. 404, 83–92. https://doi.org/10.1016/j.colsurfa.2012.04.016.

Cornelis, G., Pang, L., Doolette, C., Kirby, J.K., McLaughlin, M.J., 2013. Transport of silver nanoparticles in saturated columns of natural soils. Sci. Total Environ. 463–464, 120–130. https://doi.org/10.1016/j.scitotenv.2013.05.089.

Council, N.R., 2013. Research Progress on Environmental, Health, and Safety Aspects of Engineered Nanomaterials. The National Academies Press, Washington, DC. https://doi.org/10.17226/18475.

Davis, S.N., Thompson, G.M., Bentley, H.W., Stiles, G., 1980. Ground-water tracers - a short review. Ground Water 18, 14–23. https://doi.org/10.1111/j.1745-6584.1980.tb03366.x.

Fontes, M.P.F., Alleoni, L.R.F., 2006. Electrochemical attributes and availability of nutrients, toxic elements, and heavy metals in tropical soils. Sci. Agric. 63, 589–608.

Fontes, M.P.F., Weed, S.B., 1991. Iron oxides in selected Brazilian Oxisols: I. Mineralogy. Soil Sci. Soc. Am. J. 55 (1143) https://doi.org/10.2136/sssaj1991.03615995005500040040x.

Ginn, J.S., Russel Boulding, J., 2003. Soil and ground water tracers. In: Press, C. (Ed.), Practical Handbook of Soil, Vadose Zone, and Ground-water Contamination. CRC Press. https://doi.org/10.1201/9781420032147.ch8.

Goldberg, S., Kabengi, N.J., 2010. Bromide adsorption by reference minerals and soils. Vadose Zo. J. 9, 780–786. https://doi.org/10.2136/vzj2010.0028.

Huysmans, M., Dassargues, A., 2005. Review of the use of Péclet numbers to determine the relative importance of advection and diffusion in low permeability environments. Hydrogeol. J. 13, 895–904. https://doi.org/10.1007/s10040-004-0387-4.

IGBP-DIS, 1998. SoilData(V.0) a Program for Creating Global Soil-property Databases [WWW Document]. IGBP Glob. Soils Data Task. https://nelson.wisc.edu/sage/data-and-models/atlas/maps.php?datasetid=20&includerelatedlinks=1&dataset=20 (Accessed 5 May 2016).

Korom, S.F., Seaman, J.C., 2012. When "conservative" anionic tracers Aren't. Groundwater 50, 820–824. https://doi.org/10.1111/j.1745-6584.2012.00950.x.

Kumahor, S.K., Hron, P., Metreveli, G., Schaumann, G.E., Klitzke, S., Lang, F., Vogel, H.-J., 2016. Transport of soil-aged silver nanoparticles in unsaturated sand. J. Contam. Hydrol. 195, 31–39. https://doi.org/10.1016/j.jconhyd.2016.10.001.

Levy, B.S., Chambers, R.M., 1987. Bromide as a conservative tracer for soil-water studies. Hydrol. Process 1, 385–389. https://doi.org/10.1002/hyp.3360010406.

Li, Z., Shuman, L.M., 1997. Estimation of retardation factor of dissolved organic carbon in sandy soils using batch experiments. Geoderma 78, 197–206. https://doi.org/10.1016/S0016-7061(97)00048-7.

Maraqa, M.A., 2001. Prediction of mass-transfer coefficient for solute transport in porous media. J. Contam. Hydrol. 50, 1–19. https://doi.org/10.1016/S0169-7722(01)00107-3.

Melo, V.F., Fontes, M.P.F., Novais, R.F., Singh, B., Schaefer, C.E.G.R., 2001. Características dos óxidos de ferro e de alumínio de diferentes classes de solos. Rev. Bras. Ciência do Solo 25, 19–32. https://doi.org/10.1590/S0100-06832001000100003.

Nimmo, J.R., 2004. Porosity and Pore Size Distribution, in: Encyclopedia of Soils in the Environment. Elsevier, London, pp. 295–303.

OECD, 2004. Test No. 312. Leaching in soil columns. Guidel. Test. Chem.

OECD, 2000. Test No. 106: Adsorption – Desorption Using a Batch Equilibrium Method. OECD Publishing.

Oliviera, I.B., Demond, A.H., Salehzadeh, A., 1996. Packing of sands for the production of homogeneous porous media. Soil Sci. Soc. Am. J. 60, 49–53.

Osman, K.T., 2013. Soils: Principles, Properties and Management. Springer.

Prathna, T.C., Chandrasekaran, N., Mukherjee, A., 2011. Studies on aggregation behaviour of silver nanoparticles in aqueous matrices: effect of surface functionalization and matrix composition. Colloids Surfaces A Physicochem. Eng. Asp. 390, 216–224. https://doi.org/10.1016/j.colsurfa.2011.09.047.

Rosas Medina, A.A., 2005. El número de peclet y su significación en la modelación de transporte difusivo de contaminantes. UNAM.

Sagee, O., Dror, I., Berkowitz, B., 2012. Transport of silver nanoparticles (AgNPs) in soil. Chemosphere 88, 670–675. https://doi.org/10.1016/j.chemosphere.2012.03.055.

Selim, H.M., Amacher, M.C., 1997. Reactivity and Transport of Heavy Metals on Soils. CRC Press, Inc.

Simunek, J., van Genuchten, M.T., Genuchten, M.T. van, 2006. Contaminant transport in the unsaturated zone. In: The Handbook of Groundwater Engineering, Second Edition. CRC Press, pp. 22–46. https://doi.org/10.1201/9781420006001.ch22.

Šimůnek, J., van Genuchten, M.T., Šejna, M., 2008. Development and applications of the HYDRUS and STANMOD software packages and related codes. Vadose Zo. J. 7, 587–600. https://doi.org/10.2136/vzj2007.0077.

Singha, D., Barman, N., Sahu, K., 2014. A facile synthesis of high optical quality silver nanoparticles by ascorbic acid reduction in reverse micelles at room temperature. J. Colloid Interface Sci. 413, 37–42. https://doi.org/10.1016/j.jcis.2013.09.009.

Uraisin, K., Takayanagi, T., Oshima, M., Nacapricha, D., Motomizu, S., 2006. Kinetic-spectrophotometric method for the determination of trace amounts of bromide in seawater. Talanta 68, 951–956. https://doi.org/10.1016/j.talanta.2005.06.061.

van Genuchten, M.T., Leij, F.J., 2001. Solute transport. In: Soil Physics Companion. CRC Press, pp. 189–248. https://doi.org/10.1201/9781420041651.ch6.

Wang, D., Jaisi, D.P., Yan, J., Jin, Y., Zhou, D., 2015. Transport and retention of polyvinylpyrrolidone-coated silver nanoparticles in natural soils. Vadose Zo. J. 14.

Yaron, B., Bruno, Danfors, E., Vaadia, Y., 1973. Arid Zone Irrigation. Springer, Berlin Heidelberg.

Zaribafan, A., Haghbeen, K., Fazli, M., Akhondali, A., 2014. Spectrophotometric method for hydrogen peroxide determination through oxidation of organic dyes. Environ. Stud. Persian Gulf 1, 93–101.